Published in final edited form as:
Magn Reson Med. 2012 September ; 68(3): 703–710. doi:10.1002/mrm.23273.

Shared Velocity Encoding (SVE): A method to improve the temporal resolution of phase contrast velocity measurements

Hung-Yu Lin[1,2], **Jacob A. Bender**[1,2], **Yu Ding**[2], **Yiu-Cho Chung**[4], **Alice M. Hinton**[5], **Michael L. Pennell**[5], **Kevin K. Whitehead**[6], **Subha V. Raman**[2,3,7], and **Orlando P. Simonetti**[1,2,3,7]

[1]Department of Biomedical Engineering, The Ohio State University, Columbus, OH

[2]Dorothy M. Davis Heart & Lung Research Institute, The Ohio State University, Columbus, OH

[3]Department of Internal Medicine, Division of Cardiovascular Medicine, The Ohio State University, Columbus, OH

[4]Siemens Healthcare, Columbus, OH

[5]Division of Biostatistics, College of Public Health, The Ohio State University, Columbus, OH

[6]Children's Hospital of Philadelphia, Cardiology, Main Hospital, 2nd Floor, 34th and Civic Center Blvd, Philadelphia, PA 19104

[7]Department of Radiology, The Ohio State University, Columbus, OH

Abstract

Phase contrast magnetic resonance imaging (PC-MRI) is used routinely to measure fluid and tissue velocity with a variety of clinical applications. PC-MRI methods require acquisition of additional data to enable phase difference reconstruction, making real-time imaging problematic. Shared Velocity Encoding (SVE), a method devised to improve the effective temporal resolution of PC-MRI, was implemented in a real-time pulse sequence with segmented echo planar readout. The effect of SVE on peak velocity measurement was investigated in computer simulation, and peak velocities and total flow were measured in a flow phantom and in volunteers and compared with a conventional ECG-triggered, segmented k-space phase-contrast sequence as a reference standard. Computer simulation showed a 36% reduction in peak velocity error from 8.8% to 5.6% with SVE. A similar reduction of 40% in peak velocity error was shown in a pulsatile flow phantom. In the phantom and volunteers, volume flow did not differ significantly when measured with or without SVE. Peak velocity measurements made in the volunteers using SVE showed a higher concordance correlation (0.96) with the reference standard than non-SVE (0.87). The improvement in effective temporal resolution with SVE reconstruction has a positive impact on the precision and accuracy of real-time PC-MRI peak velocity measurements.

Keywords

phase-contrast MRI; flow quantification; real-time imaging; shared velocity encoding

INTRODUCTION

The phase shift caused by moving spins was first described in 1954 (1) and this effect was used to measure motion in seawater in 1960 (2). The technique of Phase Contrast Magnetic

Address all correspondence to: Orlando P. Simonetti, PhD, Professor of Internal Medicine and Radiology, The Ohio State University, 460 West 12th Avenue, Room 316 Biomedical Research Tower, Columbus, OH 43210, Phone: (614) 293-0739, Fax: (614) 247-8277, Orlando.Simonetti@osumc.edu.

Resonance Imaging (PC-MRI) relies on this basic principle and has served for over two decades as an important clinical diagnostic tool used primarily to measure volume flow and peak velocities in major blood vessels and through heart valves (3–5). Today, the most commonly used PC-MRI methods still follow the original approach of acquiring two gradient echo datasets with different phase sensitivities to velocity. Phase-difference reconstruction is performed on each complex image data pair to eliminate any residual nonzero phase variation due to effects other than velocity.

Current PC-MRI methods use ECG synchronization and frequently employ strategies of k-space segmentation to reduce acquisition time (6,7) to a reasonable breath-hold. However, as with any ECG triggered pulse sequence, this method requires a reliable ECG signal and regular cardiac rhythm. Signal-averaging and respiratory gating can be used to suppress respiratory motion artifacts when breath-holding is not feasible. Furthermore, the velocity information resulting from a segmented k-space acquisition is a weighted temporal average of the velocity waveform acquired over multiple cardiac and respiratory cycles; short-term hemodynamic variations are lost, such as those that occur under pharmacological stress (8,9), following physical exercise (10,11), or during other physical maneuvers (14,15). Real time PC-MRI would be desirable for these applications and as an alternative for patients with irregular cardiac rhythm or inability to breath-hold.

Whereas real-time acquisition of cine images without ECG synchronization or breath-holding is often used to evaluate cardiac function in patients when conventional ECG-triggered segmented k-space acquisitions fail, real-time PC-MRI is not commonly utilized due to its intrinsically slower acquisition rate. Various methods for real-time PC-MRI have been previously proposed, including the use of alternative k-space sampling trajectories such as gradient-echo echo-planar (12–16) and spiral readouts (17–19). While these rapid *k*-space sampling strategies have successfully demonstrated the feasibility of measuring blood flow in real time, temporal resolution remains a concern. Temporal data sharing schemes such as view-sharing are commonly used to improve effective temporal resolution in dynamic imaging, and have been demonstrated to increase the accuracy of estimation of the left ventricular end-systolic volume (20). A view-sharing scheme incorporating more frequent updating of the central lines in a segmented k-space acquisition (21) has been shown to improve the temporal resolution of PC-MRI (22). However, view-sharing alone may not be sufficient to achieve adequate temporal resolution with *real-time* velocity imaging, in particular at the high heart rates encountered during pharmacological or exercise stress testing, or when accurate peak velocity measurement is required. Additionally, any data sharing scheme must be compatible with the desired k-space trajectory (e.g., EPI, radial, spiral) and parallel imaging method (e.g., GRAPPA, TSENSE). View-sharing methods, EPI, and parallel imaging can each place competing requirements on k-space trajectories. View sharing requires flexible phase-encoding line ordering while EPI uses blipped phase-encoding gradients to step through k-space, making practical combinations of these two methods potentially unworkable.

In the present work, a simple method originally described by Bernstein (23) that we call Shared Velocity Encoding (SVE) (23,24) is investigated as a means to improve the effective temporal resolution of PC-MRI. Unlike view-sharing, SVE shares velocity encodings, rather than portions of k-space, between adjacent frames resulting in a doubling of the effective temporal resolution. The method does not impose specific requirements on the k-space trajectory and therefore works seamlessly with EPI and parallel imaging under-sampling strategies. The aim of the present work is to investigate and demonstrate the advantages and tradeoffs of the SVE method applied to real-time PC-MRI. Computer simulations are used to investigate the impact of SVE on the precision of peak velocity measurement, a pulsatile flow phantom is used to evaluate the accuracy of real-time flow and peak velocity

measurements, and experiments in normal human subjects are used to demonstrate the feasibility and effectiveness of real-time PC-MRI utilizing SVE.

THEORY

PC-MRI is typically performed using one of two methods: one-sided encoding (Figure 1a) in which velocity compensated and velocity encoded data are acquired for each cardiac phase(25), or two-sided encoding (Figure 1b) in which data with equal and opposite velocity encodings are acquired (26,27). The SVE concept, illustrated in Figure 1d, is to share one version of velocity encoded k-space data (k_+ or k_-) between adjacent frames in two-sided velocity encoded PC-MRI. In Figure 1d, the odd-numbered frames are identical to the four frames generated by conventional phase contrast reconstruction (Figure 1b); SVE additionally intermediate frames (even frames 2, 4, and 6). While each of these additional (even) frames shares velocity data with the adjacent frames, each contains a unique set of data that represents a velocity measurement centered at the time between the original frames. Thus, SVE neither interpolates data between the original frames, nor alters the temporal window used to sample the flow information. Instead, it uses a sliding window that advances one full k-space at a time, rather than shifting two full datasets between reconstructed frames as is done conventionally. SVE can also be applied to segmented acquisitions, in which case each block in the figures would represent a segment of k-space, rather than all k-space lines.

Figure 1c illustrates why the SVE method can only be used with two-sided velocity encoding. In one-sided encoding, there is no velocity information in the velocity compensated data; the SVE strategy of shifting only one k-space block at a time would result in new velocity information in only every second reconstructed image; adjacent frames would carry identical velocity information, as illustrated in Figure 1c.

The intention of the SVE reconstruction scheme is therefore to restore temporal resolution that is typically lost in two-sided PC-MRI by boosting the effective temporal resolution by a factor of two. It should be noted that while SVE doubles the effective frame rate, comparing Figure 1b and Figure 1d reveals that the temporal window of each frame is unchanged with SVE reconstruction.

METHODS

Sequence Implementation

Real-time gradient-echo echo-planar imaging (GRE-EPI) with SVE reconstruction was implemented on a 1.5T MR system with 32 receiver channels and maximum gradient amplitude and slew rate of 45 mT/m and 200 mT/m/ms respectively (MAGNETOM Avanto, Siemens Healthcare, Malvern, PA). The GRE-EPI sequence was implemented with echo train length = 15, a center-out k-space acquisition order to minimize effective echo time (TE), and through-plane velocity encoding as illustrated in Figure 2. A 25° rapid binomial water excitation pulse (28) was used in conjunction with the EPI readout to provide the fat suppression needed to avoid off-resonance artifacts. This resulted in a TE of 3.9 ms (measured from the first pulse of the 1-1 binomial water excitation pulse) and a repetition time (TR) of 13.75 ms at a VENC of 150cm/s. Four shots per image were used to collect a total of 60 k-space lines resulting in an acquisition time of 55 ms for each full k-space dataset. Parallel imaging technique TGRAPPA (29) with acceleration rate 2 was used to reconstruct 120 lines per image. Other imaging parameters used were: 2405 Hz/pixel readout bandwidth, 120 × 160 pixel reconstructed matrix, 10 mm slice, 300mm × 400mm rectangular field-of-view (2.5mm × 2.5mm pixels). Maxwell correction was used to account

for the effect of concomitant gradients on the phase maps (30). A summary of imaging parameters is given in Table 1.

Computer Simulation

Simulations were performed to confirm that the expected improvement in temporal resolution with SVE yields a more accurate measurement of peak velocity. A velocity waveform was designed to approximate systolic aortic flow at a heart rate of 75 beats per minute (800 ms R-R interval). The waveform consisted of a 300 ms half-sine wave followed by zero velocity for the remainder of the simulated RR interval (see Figure 3a). Acquisition of k-space data for a single velocity encoding was assumed to take 50ms; this can be considered as the time to acquire complete image data in the case of real-time imaging, or one segment of k-space in a segmented acquisition. Two-sided encoding was simulated for both SVE and non-SVE reconstruction. The alignment between sample points and the velocity peak was varied and peak velocity calculated over a range of time shifts of the sampling raster to investigate the influence of SVE on the average and maximum variability in measured peak velocity.

Phantom

A pulsatile phantom was used to compare SVE with conventional non-SVE reconstruction. The phantom consisted of rigid pipe with a 0.52″ inner diameter and 0.84″ outer diameter connected by flexible tubing to a Cardioflow 5000 system (Shelley Medical Imaging Technologies, London Ontario, Canada). The pipe was positioned along the length of the magnet bore passing through a transverse imaging slice at magnet isocenter. The servo motor established a cyclical flow waveform consisting of a 512ms half sine wave with a peak flow of 100ml/s followed by 512ms of no flow. A transit time ultrasound flowmeter (Transonic Systems Inc., Ithaca, NY) with the flow probe (ME19PXN) positioned between the pump and the imaged slice, at the junction of the flexible tubing and the rigid pipe, was used to record and verify the MRI flow measurements.

Volunteers

This study was approved by our institutional review board (IRB) and was compliant with the Health Insurance Portability and Accountability Act (HIPAA). Informed consent was obtained from all volunteers. Thirteen healthy volunteers (mean age 32.5 ± 12.5 years, range 19 to 56; 3 female) with no history of cardiovascular disease were scanned. Through-plane velocity measurements were made in each volunteer in the ascending aorta and main pulmonary artery (MPA) immediately distal to the valve at the valve leaflet tips. Multiple scout planes were used to ensure the velocity measurement planes were perpendicular to the vessels of interest. Three measurements were made in each vessel. The first and third measurements utilized a conventional, retrospectively-gated, segmented k-space PC-MRI acquisition which were averaged to account for physiological drift. This is the same pulse sequence and scan parameters used in our clinical cardiac MRI lab for velocity measurements. The second acquisition in each vessel utilized the real-time PC-MRI sequence. Real-time data were acquired over approximately ten cardiac cycles and the volunteers were instructed to breath-hold to ensure registration with the segmented k-space acquisitions. Acquisition parameters (see Table 1) including spatial resolution and temporal resolution were matched as closely as possible between the segmented k-space and real-time acquisitions. The real-time sequence used two-sided velocity encoding to enable SVE reconstruction; the segmented breath-hold scan utilized the standard PC-MRI gradient echo sequence available on the scanner which incorporated one-sided encoding. The real-time data was reconstructed both with and without SVE for comparison.

Flow and Peak Velocity Analysis – Phantom and Volunteer Data

The measurement methods described here were used for both the phantom and the volunteer data. ROIs were drawn on the vessels of interest in the PC-MRI cines and image analysis was done using the freely available software Segment version 1.8 (31). Peak velocity and total flow over the cardiac cycle were measured. From the real-time data, the peak velocity was manually selected for each heartbeat and then averaged over all cardiac cycles for the purpose of comparing with the segmented k-space sequence that results in a single measurement of peak velocity and flow volume for each scan.

The phantom data were analyzed with non-parametric methods due to the non-normality of the data (as indicated by normal-quantile plots) SVE and non-SVE flow or velocity measurements were compared to the reference standard through Wilcoxon's signed rank test and also compared to one another through Wilcoxon's rank sum test. SVE and non-SVE flow measurements were compared to ultrasound flow using Wilcoxon's signed rank test.

The SVE and non-SVE flow and peak velocity measurements on the 13 volunteers were compared to the reference standard segmented acquisition using concordance correlation coefficients (CCCs) and Bland-Altman plots. The CCC measures how closely the SVE/non-SVE measurements adhere to a 45 degree line (i.e., a line of perfect agreement) when plotted against the reference standard values, with a value of 1 denoting perfect agreement. Each analysis required methods to account for correlations between the aorta and MPA measurements on the same subject. Limits of agreement (bias ± 1.96 s.d.) for the Bland-Altman analysis were calculated using Bland and Altman's formula for repeated measures data (32) while CCCs and their confidence intervals were calculated using King, Chinchilli, and Carrasco's method for repeated measures data (33).

RESULTS

Computer Simulation

Figure 3b illustrates the measured peak velocity as a function of the temporal offset between sample points and the true peak. The results show that both SVE and non-SVE reconstructions underestimated the peak velocity at any offset between the peak and sample points due to the implicit temporal averaging of a finite temporal window. For smaller offsets, SVE and non-SVE showed identical performance; however, when the offset increased, the additional frames generated by the SVE reconstruction were able to more accurately capture the peak velocity and reduce the peak velocity error compared to conventional (non-SVE) reconstruction. SVE showed a 36% reduction in peak velocity error *on average* (SVE: 5.59%, non-SVE: 8.81%), and reduced the maximum potential error caused by temporal misregistration of the velocity peak with sample points by 55% (SVE: 7.76%, non-SVE: 17.30%). Numerical results are listed in Table 2.

Phantom

The two-sided velocity-encoded real-time data was acquired over nine pulsatile cycles. These were compared to the reference standard obtained using the standard segmented k-space acquisition, and also to flow measured using the ultrasound flow probe. The median phantom flow measured using SVE reconstruction (26.96 ml/s) was closer to the reference standard flow (26.24 ml/s) than non-SVE (22.57 ml/s), though neither median was significantly different from reference standard ($p = 0.16$ for SVE and $p = 0.43$ for non-SVE) and the measurements were not significantly different from one another ($p = 1.00$). The median SVE flow was significantly ($p = 0.004$) less than ultrasound flow (32.07 ml/s). Although there was a greater difference between the median non-SVE flow and the ultrasound flow, statistical significance was not achieved ($p = 0.10$) due to the high

variability in the measurements (range = 21.74 – 33.66 ml/s). The median peak velocity measured using SVE (96.39 cm/s) was not significantly different from the reference standard peak velocity of 97.85 cm/s ($p = 0.18$). The median non-SVE peak velocity (95.43 cm/s), on the other hand, was significantly lower than reference standard ($p = 0.04$), although it was not significantly different from the median SVE peak velocity ($p = 0.14$).

Volunteers

Six measurements (real-time SVE, real-time non-SVE, plus the reference standard technique for both aorta and MPA) were reconstructed in each of the 13 volunteers for a total of 78 velocity waveforms. The number of cardiac cycles for individual real-time scans ranged from 8 to 15 with a mean of 11.1. Example magnitude and phase images and the resulting aortic velocity waveforms from each of the measurements in a single volunteer are illustrated in Figure 4.

SVE and non-SVE measurements were compared to the reference standard using the concordance correlation coefficient (CCC). SVE and non-SVE measurements of flow demonstrated similar agreement with the reference standard: the estimated CCCs were close to one another (0.72 for SVE and 0.71 for non-SVE) and there was a significant amount of overlap in their 95% confidence intervals ((0.54, 0.84) for SVE and (0.52, 0.83) for non-SVE). In contrast, the CCC comparing SVE peak velocity with the reference standard (0.96) was considerably larger than the CCC comparing non-SVE peak velocity to the reference standard (0.87) and there was no overlap in their 95% confidence intervals ((0.95, 0.98) for SVE and (0.78, 0.93) for non-SVE), indicating that the SVE peak velocity results more closely match those of the reference standard.

Agreement with reference standard was also assessed using Bland-Altman plots (Figures 5 and 6). As seen in Figure 5, SVE and non-SVE measurements of flow exhibited similar levels of bias (−8.93 and −9.49 respectively) and limits of agreement: −27.82 to 9.97 for SVE and −28.03 to 9.06 for non-SVE. However, as seen in the CCC analysis, SVE and non-SVE peak velocity measurements exhibited different levels of agreement with reference standard; as seen in Figure 6, SVE measurements of peak velocity were less biased (0.46 compared to −5.08) and exhibited a narrower agreement interval: −10.07 to 10.98 for SVE and −20.32 to 10.16 for non-SVE.

DISCUSSION

We have shown that the improvement in the effective temporal resolution of real-time PC-MRI provided by SVE reconstruction resulted in peak velocity measurements comparable to the conventional segmented k-space acquisition that served as the reference standard. The segmented acquisition had an acquired true temporal resolution equivalent to the effective temporal resolution of the real-time sequence using SVE. The results demonstrated in flow phantom and volunteers were supported by the computer simulation showing that SVE reconstruction improved peak velocity accuracy when compared with standard reconstruction. Both SVE and non-SVE somewhat underestimated the peak velocity due to the temporal averaging inherently caused by the finite length (110 ms) temporal sampling window. The measured peak velocity was also sensitive to the temporal alignment of the acquired sample points with the instant the peak velocity occurs. The simulation showed that when the peak velocity fell between temporal sample points, it was more severely underestimated. The intermediate frames generated by SVE improved the precision of peak velocity measurements by reducing the maximum potential misalignment between the center of the temporal window and the time of the velocity peak. On average, SVE yielded a more accurate and less variable peak velocity than conventional reconstruction of two-sided encoded PC-MRI data. Reduced variability is expected to enhance the reliability of peak

velocity measurements and to improve the evaluation of physiological beat-to-beat variability in volume flow and velocity. In phantom, and volunteer studies, SVE results showed a significantly higher concordance correlation with the reference standard than non-SVE, which tended to underestimate peak velocity as expected from the simulation results. These results indicate that SVE should be the reconstruction method of choice when two sided velocity encoding is employed. SVE fully utilizes the velocity information already encoded into the k-space data set by combining the alternately velocity encoded data set in a sliding window fashion.

While measurement of peak velocity can be greatly affected by temporal resolution, volume flow measurement involves integration of flow over the entire cardiac cycle and may not be as sensitive to it. The flow phantom showed similar volume flow for the reference standard, SVE, and non-SVE techniques, although all three MRI methods yielded flow measurements lower than the ultrasound flow probe. In volunteers, flow volumes generated using SVE and non-SVE reconstructed data agreed well with one another but were nearly 10 ml/s lower than the reference standard segmented acquisition. One possible source of this underestimation is the intrinsic sensitivity of flow measurement to small background phase offsets. As recently pointed out by Gatehouse et al. (34), even small background phase errors of the order of 1 or 2 cm/s can corrupt volume flow measurements which are based on the integration of velocities across the entire cross sectional area of the vessel and across all phases of the cardiac cycle. The use of a segmented echo planar readout with rapid gradient switching may contribute to greater eddy current generated phase offsets, but this was not investigated.

A unique advantage of SVE over conventional view-sharing methods is that it can be easily combined with existing k-space trajectories and undersampling strategies such as EPI and TSENSE as shown in this study. SVE is a reconstruction technique and could be combined with conventional echo-sharing to further improve temporal resolution. Note that the concept of SVE can also be extended to multi-directional flow-encoding. For the balanced four point encoding scheme that is often used to encode velocity in x, y, and z directions (26), the effective temporal resolution could potentially be increased by a factor of four using SVE, since each of the encodings are sensitive to velocity and could be shared using a sliding-window type reconstruction.

Limitations

It is expected that EPI acquisition may be more sensitive to eddy-current induced phase offsets; this may explain the difference in flow measured using the EPI sequence (SVE or non-SVE) compared to the conventional gradient echo standard. Our primary interest was in the effect of SVE on temporal resolution, which mainly impacts peak velocity measurements; as such, background phase offsets were not investigated or corrected in this study. A recognized limitation of two-sided versus one-sided velocity encoding is that two-sided encoding lacks a flow-compensated image; therefore magnitude images must be reconstructed using velocity-sensitized data and may be more sensitive to flow artifacts. However, given that quantitative velocity measurements are the prime objective of PC-MRI, this is of limited significance. It should also be noted that only healthy volunteers with normal velocities and normal heart rates were included in the study; imaging large vessels in normal adult subjects places relatively low demands on spatial and temporal resolution. The segmented k-space gradient echo sequence used as the reference standard can be configured to run with higher spatial and temporal resolution than was utilized, although at the expense of longer breath-hold duration. Higher spatial and temporal resolution would be required in patients with higher velocity blood flow, such as children with congenital heart disease and patients with stenotic valves and high jet velocities. It will be important to investigate the

accuracy of peak velocity measurements using the real-time sequence in these and other patient populations in the future.

Conclusion

The SVE reconstruction method demonstrated real gains in temporal resolution that resulted in more accurate peak velocity measurements. With SVE reconstruction, real-time velocity measurement becomes practical with the temporal resolution approaching that of conventional segmented PC-MRI. SVE enables real-time velocity imaging that is not limited by patient cooperation or breath-holding abilities, or regular cardiac rhythm, and is expected to become an important clinical imaging tool.

Acknowledgments

The project described was partially supported by Award Number R01HL102450 from the National Heart, Lung, And Blood Institute. The content is solely the responsibility of the authors and does not necessarily represent the official views of the National Heart, Lung, and Blood Institute or the National Institutes of Health.

References

1. Carr HY, Purcell EM. Effects of diffusion on free precession in nuclear magnetic resonance experiments. Phys Rev. 1954; 94:630–638.
2. Hahn EL. Detection of sea-water motion by nuclear precession. J Geophys Res. 1960; 65:776–777.
3. Bryant DJ, Payne JA, Firmin DN, Longmore DB. Measurement of flow with NMR imaging using a gradient pulse and phase difference technique. J Comput Assist Tomogr. 1984; 8(4):588–593. [PubMed: 6736356]
4. Moran PR. A flow velocity zeugmatographic interlace for NMR imaging in humans. Magn Reson Imaging. 1982; 1(4):197–203. [PubMed: 6927206]
5. van Dijk P. Direct cardiac NMR imaging of heart wall and blood flow velocity. J Comput Assist Tomogr. 1984; 8(3):429–436. [PubMed: 6725689]
6. Chatzimavroudis GP, Zhang H, Halliburton SS, Moore JR, Simonetti OP, Schvartzman PR, Stillman AE, White RD. Clinical blood flow quantification with segmented k-space magnetic resonance phase velocity mapping. J Magn Reson Imaging. 2003; 17(1):65–71. [PubMed: 12500275]
7. Edelman RR, Manning WJ, Gervino E, Li W. Flow velocity quantification in human coronary arteries with fast, breath-hold MR angiography. J Magn Reson Imaging. 1993; 3(5):699–703. [PubMed: 8400554]
8. Davis CP, Liu PF, Hauser M, Gohde SC, von Schulthess GK, Debatin JF. Coronary flow and coronary flow reserve measurements in humans with breath-held magnetic resonance phase contrast velocity mapping. Magn Reson Med. 1997; 37(4):537–544. [PubMed: 9094075]
9. Grist TM, Polzin JA, Bianco JA, Foo TK, Bernstein MA, Mistretta CM. Measurement of coronary blood flow and flow reserve using magnetic resonance imaging. Cardiology. 1997; 88(1):80–89. [PubMed: 8960630]
10. Pedersen EM, Kozerke S, Ringgaard S, Scheidegger MB, Boesiger P. Quantitative abdominal aortic flow measurements at controlled levels of ergometer exercise. Magn Reson Imaging. 1999; 17(4):489–494. [PubMed: 10231175]
11. Hjortdal VE, Emmertsen K, Stenbog E, Frund T, Schmidt MR, Kromann O, Sorensen K, Pedersen EM. Effects of exercise and respiration on blood flow in total cavopulmonary connection: a real-time magnetic resonance flow study. Circulation. 2003; 108(10):1227–1231. [PubMed: 12939218]
12. Korperich H, Gieseke J, Barth P, Hoogeveen R, Esdorn H, Peterschroder A, Meyer H, Beerbaum P. Flow Volume and Shunt Quantification in Pediatric Congenital Heart Disease by Real-Time Magnetic Resonance Velocity Mapping: A Validation Study. Circulation. 2004; 109(16):1987–1993. [PubMed: 15066942]

13. Debatin JF, Leung DA, Wildermuth S, Botnar R, Felblinger J, McKinnon GC. Flow quantitation with echo-planar phase-contrast velocity mapping: in vitro and in vivo evaluation. J Magn Reson Imaging. 1995; 5(6):656–662. [PubMed: 8748482]
14. Eichenberger AC, Schwitter J, McKinnon GC, Debatin JF, von Schulthess GK. Phase-contrast echo-planar MR imaging: real-time quantification of flow and velocity patterns in the thoracic vessels induced by Valsalva's maneuver. J Magn Reson Imaging. 1995; 5(6):648–655. [PubMed: 8748481]
15. Firmin DN, Klipstein RH, Hounsfield GL, Paley MP, Longmore DB. Echo-planar high-resolution flow velocity mapping. Magn Reson Med. 1989; 12(3):316–327. [PubMed: 2628682]
16. McKinnon GC, Debatin JF, Wetter DR, von Schulthess GK. Interleaved echo planar flow quantitation. Magn Reson Med. 1994; 32(2):263–267. [PubMed: 7968452]
17. Gatehouse PD, Firmin DN, Collins S, Longmore DB. Real time blood flow imaging by spiral scan phase velocity mapping. Magn Reson Med. 1994; 31(5):504–512. [PubMed: 8015403]
18. Nezafat R, Kellman P, Derbyshire JA, McVeigh ER. Real-time blood flow imaging using autocalibrated spiral sensitivity encoding. Magn Reson Med. 2005; 54(6):1557–1561. [PubMed: 16254954]
19. Park JB, Olcott EW, Nishimura DG. Rapid measurement of time-averaged blood flow using ungated spiral phase-contrast. Magn Reson Med. 2003; 49(2):322–328. [PubMed: 12541253]
20. Foo TK, Bernstein MA, Aisen AM, Hernandez RJ, Collick BD, Bernstein T. Improved ejection fraction and flow velocity estimates with use of view sharing and uniform repetition time excitation with fast cardiac techniques. Radiology. 1995; 195(2):471–478. [PubMed: 7724769]
21. Laub, G. Breath-hold cine MR imaging with a shared and reordered gradient echo technique. New York, New York: 1993. p. 478
22. Markl M, Hennig J. Phase contrast MRI with improved temporal resolution by view sharing: k-space related velocity mapping properties. Magn Reson Imaging. 2001; 19(5):669–676. [PubMed: 11672625]
23. Bernstein, MA.; Foo, TK. General Electric Company, assignee. MRA image produced by temporal data sharing. USA patent 5,435,303. 1995 Jul 25. p. 1995
24. Lin H, Ding Y, Chung YC, Simonetti OP. Shared Velocity Encoding (SVE): a new method for real-time velocity measurement with high temporal resolution. Journal of Cardiovascular Magnetic Resonance. 2009; 11(Supplement 1):O81.
25. Hausmann R, Lewin JS, Laub G. Phase-contrast MR angiography with reduced acquisition time: new concepts in sequence design. J Magn Reson Imaging. 1991; 1(4):415–422. [PubMed: 1790363]
26. Dumoulin CL, Souza SP, Darrow RD, Pelc NJ, Adams WJ, Ash SA. Simultaneous acquisition of phase-contrast angiograms and stationary-tissue images with Hadamard encoding of flow-induced phase shifts. J Magn Reson Imaging. 1991; 1(4):399–404. [PubMed: 1790361]
27. Bernstein MA, Shimakawa A, Pelc NJ. Minimizing TE in moment-nulled or flow-encoded two- and three-dimensional gradient-echo imaging. J Magn Reson Imaging. 1992; 2(5):583–588. [PubMed: 1392252]
28. Lin HY, Raman SV, Chung YC, Simonetti OP. Rapid phase-modulated water excitation steady-state free precession for fat suppressed cine cardiovascular MR. J Cardiovasc Magn Reson. 2008; 10:22. [PubMed: 18477396]
29. Breuer FA, Kellman P, Griswold MA, Jakob PM. Dynamic autocalibrated parallel imaging using temporal GRAPPA (TGRAPPA). Magn Reson Med. 2005; 53(4):981–985. [PubMed: 15799044]
30. Bernstein MA, Zhou XJ, Polzin JA, King KF, Ganin A, Pelc NJ, Glover GH. Concomitant gradient terms in phase contrast MR: analysis and correction. Magn Reson Med. 1998; 39(2):300–308. [PubMed: 9469714]
31. Heiberg E, Sjogren J, Ugander M, Carlsson M, Engblom H, Arheden H. Design and validation of Segment--freely available software for cardiovascular image analysis. BMC Med Imaging. 2010; 10:1. [PubMed: 20064248]
32. Bland JM, Altman DG. Statistical methods for assessing agreement between two methods of clinical measurement. Lancet. 1986; 1(8476):307–310. [PubMed: 2868172]

33. King TS, Chinchilli VM, Carrasco JL. A repeated measures concordance correlation coefficient. Stat Med. 2007; 26(16):3095–3113. [PubMed: 17216594]

34. Gatehouse PD, Rolf MP, Graves MJ, Hofman MB, Totman J, Werner B, Quest RA, Liu Y, von Spiczak J, Dieringer M, Firmin DN, van Rossum A, Lombardi M, Schwitter J, Schulz-Menger J, Kilner PJ. Flow measurement by cardiovascular magnetic resonance: a multi-centre multi-vendor study of background phase offset errors that can compromise the accuracy of derived regurgitant or shunt flow measurements. J Cardiovasc Magn Reson. 12:5. [PubMed: 20074359]

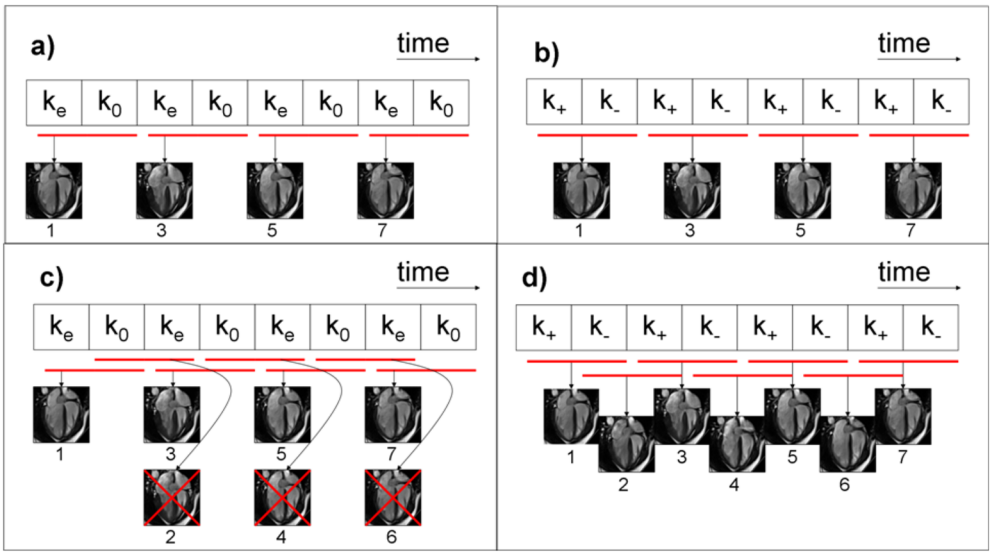

Figure 1.

The top two diagrams illustrate conventional one-sided (a) and two-sided (b) velocity encoding. The red bars in all diagrams show the data included in the reconstruction of each frame. One-sided velocity encoding (a) utilizes pairs of velocity encoded (k_e) and velocity compensated (k_0) k-space data. Two-sided encoding utilizes k-space data pairs with positive (k+) and negative (k−) velocity sensitivities (b). The proposed method of shared velocity encoding (SVE) image reconstruction is illustrated in (d). SVE cannot be combined with one-sided encoding as shown in (c) since image pairs sharing the same velocity encoded data (k_e) would be redundant.

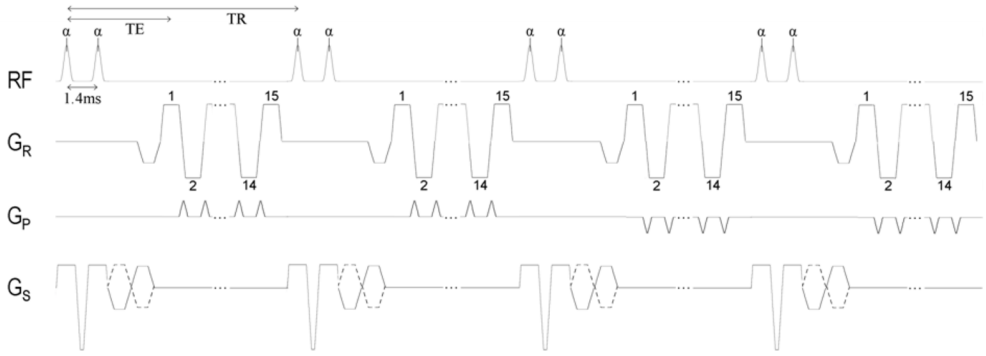

Figure 2.
Pulse sequence diagram illustrating details of the segmented EPI acquisition with velocity encoding on the slice-select gradient axis. Center-out encoding is used for every echo train. The diagram accurately depicts the sequence timing used in this study, although only 2 of the 4 shots used for each image are shown. Echo train length of 15, 4 shots per image, and TGRAPPA acceleration factor of 2 resulted in 120 reconstructed lines.

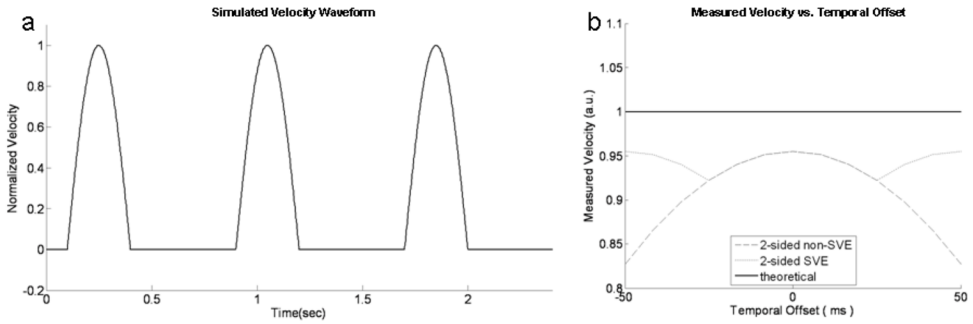

Figure 3.

On the left (a) is a plot of simulated aortic velocity vs. time. The velocity is modeled with a half wave sine with R-R interval = 800ms and pulse duration = 300ms. Graph on the right (b) shows the results of theoretical, SVE, and non-SVE peak velocity measurements over a range of temporal offsets expressed in milliseconds relative to simulated half sine wave. The error function is periodic.

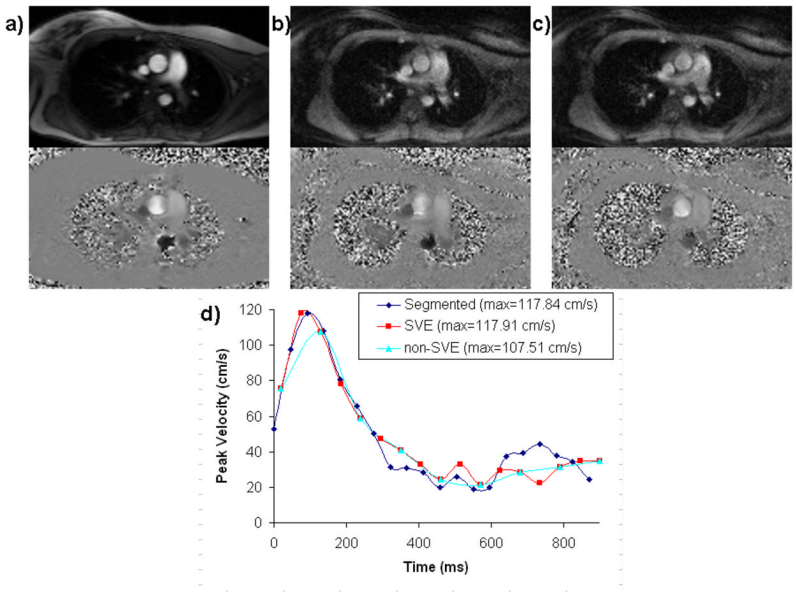

Figure 4.

Example magnitude and phase-velocity images for segmented k-space (a), real time non-SVE (b), and real time SVE (c) of the thoracic aorta in a volunteer showing typical image quality. Aortic velocity waveforms are shown from one volunteer acquired using segmented k-space, real-time SVE, and real-time non-SVE (d). Note the degradation in peak velocity when real-time acquisition is used without SVE reconstruction.

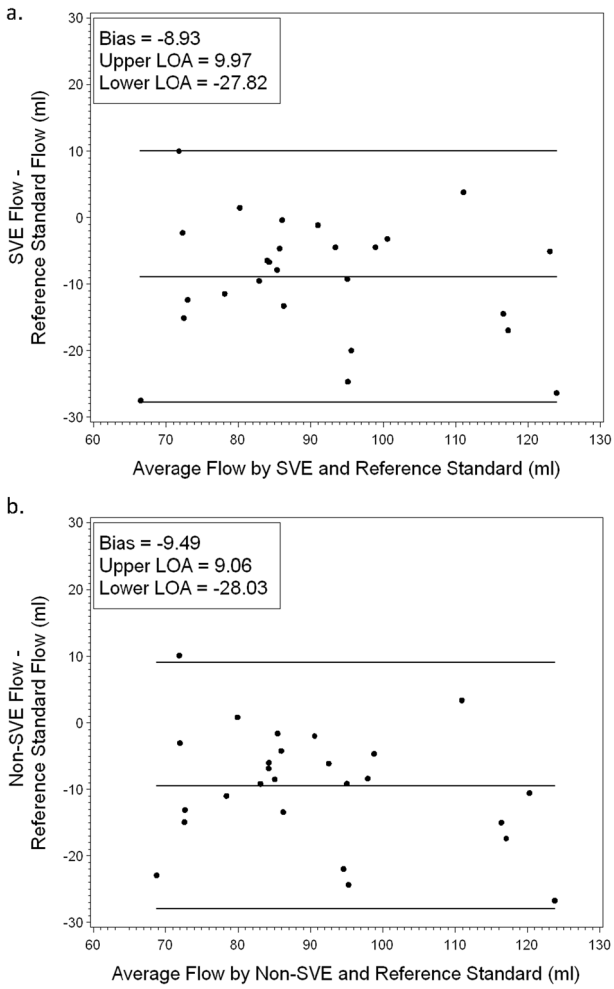

Figure 5.
Bland-Altman plot of flow for reference standard versus SVE (a) and reference standard versus non-SVE (b). Both SVE and non-SVE show similar bias in flow measurements.

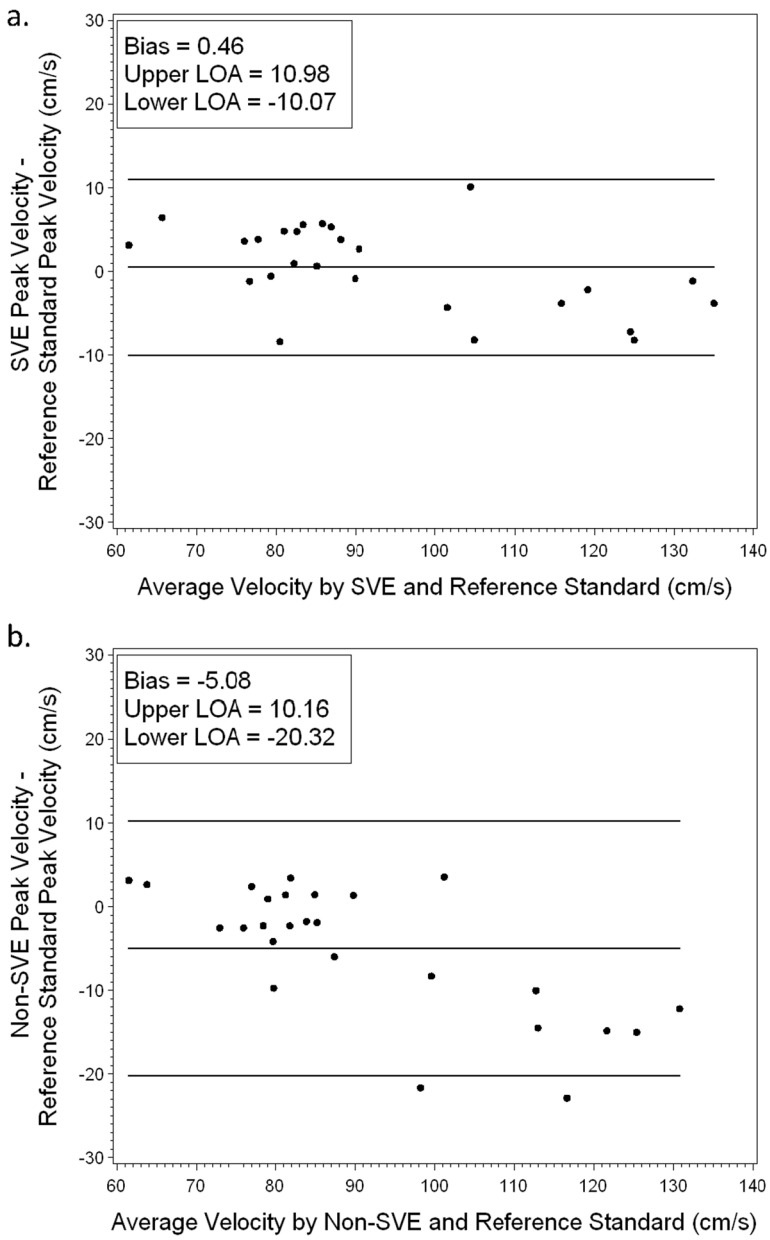

Figure 6.
Bland-Altman plot of peak velocity for reference standard versus SVE (a) and reference standard versus non-SVE (b). SVE shows reduced bias in peak velocity measurements compared to non-SVE.

Table 1

Imaging parameters used for phantom and volunteer scans.

	Reference Standard (segmented)	SVE and non-SVE (real time)
Temporal Resolution (ms)	55	55 (SVE) 110 (non-SVE)
VENC (cm/s)	150	
Parallel Acceleration	2×	
Flip Angle	25°	
Acquisition	Segmented Gradient Echo 5 lines per segment	Real Time Gradient Echo EPI 4 shots per image
Echo Train Length	1	15
Read Direction		
FOV (mm)	400	
Pixel Number	160	
Pixel Size (mm)	2.5	
Bandwidth (Hz/pixel)	600	2405
Phase Direction		
FOV (mm)	300	
Pixel Number	120	
Pixel Size (mm)	2.5	
TR	4.6 ms	13.75 ms
TE	2.0 ms	2.5ms

Table 2

Computer simulation error in peak velocity measurement expressed as percentages of true peak velocity.

	non-SVE	SVE
minimum error	4.51%	4.51%
maximum error	17.30%	7.76%
error range	12.79%	3.25%
average error	8.81%	5.59%